High-order harmonic generation by atoms in a few-cycle laser pulse: Carrier-envelope phase and many-electron effects

M. V. Frolov, N. L. Manakov, A. A. Silaev, N. V. Vvedenskii, and Anthony F. Starace

Phys. Rev. A **83**, 021405 — Published 25 February 2011

DOI: 10.1103/PhysRevA.83.021405

High Harmonic Generation by Atoms in a Few-Cycle Laser Pulse: Carrier-Envelope Phase and Many-Electron Effects

M. V. Frolov,[1] N. L. Manakov,[1] A. A. Silaev,[2] N. V. Vvedenskii,[2] and Anthony F. Starace[3]

[1] *Department of Physics, Voronezh State University, Voronezh 394006, Russia*
[2] *Institute of Applied Physics, Russian Academy of Sciences, Nizhny Novgorod 603950, Russia*
[3] *Department of Physics and Astronomy, The University of Nebraska, Lincoln NE 68588-0299, USA*

Analytic formulas describing high harmonic generation (HHG) by atoms in a short laser pulse are obtained quantum mechanically in the tunneling limit. These results provide analytic expressions of the three-step HHG scenario, as well as of the returning electron wave packet, in a few-cycle pulse. Our results agree well with those of numerical solutions of the time-dependent Schrödinger equation for the H atom, while for Xe they predict many-electron atomic dynamics features in few-cycle HHG spectra and significant dependence of these features on the carrier-envelope phase of a laser pulse.

PACS numbers: 42.65.Ky; 32.80.Rm

Extremely short (few cycle) laser pulses are presently available for high harmonic generation (HHG) experiments [1]. For such pulses, HHG spectra are highly sensitive to the electric field vector of the pulse, which for the case of linear polarization may be parameterized as:

$$\mathbf{F}(t) = \hat{\mathbf{z}} F(t) = \hat{\mathbf{z}} f(t) \cos(\omega t + \phi), \tag{1}$$

where $f(t)$ is the pulse envelope (with its maximum at $t = 0$), ω is the fundamental (carrier) frequency, and ϕ is the so-called carrier-envelope phase (CEP). Although the three-step scenario [2] remains applicable for understanding HHG by atoms in a short pulse, important differences from the monochromatic field case appear for few-cycle laser pulses. First, the HHG emission becomes very broad spectrally, forming a (quasi) continuous spectrum, so that instead of HHG rates it is more appropriate to use the spectral density of radiation, $\rho(E_\Omega)$, where $E_\Omega = \hbar\Omega$ is the harmonic photon energy. Second, the shape of $\rho(E_\Omega)$ for a rapidly-varying pulse envelope, $f(t)$, becomes sensitive to the CEP, requiring an analysis of subcycle dynamics for a proper description.

The significant CEP dependence of a short-pulse HHG process has been established both experimentally and theoretically [3–10]. The most significant differences were found in the shape and the plateau-cutoff behavior of HHG spectra for *single-cycle* "sine" ($\varphi = \pi/2$) and "cosine" ($\varphi = 0$) pulses. Theoretical analyses of few-cycle pulse HHG spectra are based primarily on numerical solutions of the time-dependent Schrödinger equation (TDSE) [3, 5, 6, 8, 9] or on the use of the Lewenstein *et al.* model [11] and its modifications. However, there are as yet no closed-form formulas for $\rho(E_\Omega)$ providing an analytic description of the short-pulse HHG spectrum similar to that for a monochromatic pulse [12].

Another open question is the validity for the case of a few-cycle pulse of the phenomenological parametrization [13] of the HHG yield in terms of the photorecombination cross section (PRCS) $\sigma^{(r)}$ (which describes the final step of the three-step scenario) and the "electron wave packet" (EWP) (which describes the ionization of an atomic electron and its propagation in the laser field). This parametrization is attractive since (i) it is valid for harmonics with energies in the region of the HHG plateau cutoff, which are precisely the ones used to produce attosecond pulses, and (ii) it involves a field-free atomic parameter $\sigma^{(r)}$ that describes atomic structure effects on HHG spectra [12–16]. However, the explicit form of the EWP is known only for monochromatic [12] and two-color [15] fields, while the possible manifestation of atomic structure features in the few-cycle regime and their modification by CEP effects remain unexplored.

In this Rapid Communication we present closed-form formulas for the spectral density of radiation, $\rho(E_\Omega)$, generated by atoms in a short laser pulse. These results justify the factorization for $\rho(E_\Omega)$, provide an explicit form for the CEP-dependent EWP, and an analytic theoretical explanation for the CEP-effects and two kinds of interference features (both large-scale and fine-scale oscillations) in HHG spectra. For the H atom, our TDSE results for a single-cycle pulse confirm the high accuracy of the analytic formulas, while for inert gases we predict that atomic structure (including many-electron) features in short pulse HHG spectra are significantly modified by CEP effects and can enhance the HHG yield by an order of magnitude in atom-specific intervals of the energy E_Ω.

To describe HHG in a short laser pulse, we generalize the techniques used to obtain our *ab initio* quantum description of HHG in a monochromatic field [17] to the case of an infinite train of short pulses separated in time by $\mathcal{T}$. Each pulse of this train is the same as for an actual short laser pulse of duration τ ($\tau < \mathcal{T}$). Owing to the periodicity in time (with period $\mathcal{T}$) of such a pulse train, we can employ the quasistationary quasienergy state approach (cf., e.g., Ref. [18]) to treat the nonlinear interactions of the train with an atomic system. In this approach, the HHG amplitude is expressed in terms of the complex quasienergy of an active atomic electron [17]. For an electron in a short-range potential, this amplitude can be presented (using time-dependent effective range theory [19]) in analytic form in the tunneling limit [20]. This latter result can then be straightforwardly generalized to the case of an active atomic electron [12]. Having

thus an explicit expression for the HHG amplitude for the pulse train, the result for a *single* short pulse follows by taking the limit $\mathcal{T} \to \infty$ for fixed τ.

Our analysis shows that the HHG amplitude for a short pulse can be presented as a sum of amplitudes, $\mathcal{A}_j$, describing the generation of radiation by electrons ionized at each (jth) optical half-cycle of the pulse. The temporal integrals (involving the Green function for a free electron in a short laser pulse) in these amplitudes can be estimated using a modified saddle-point analysis, as done similarly in Refs. [15, 20]. As a result, the amplitudes $\mathcal{A}_j$ depend on the ionization ($t_i^{(j)}$) and recombination ($t_r^{(j)}$) times for the jth *half-cycle* [where $t_r^{(j)}$ lies in the $(j+1)$th half-cycle]. These times satisfy the system of classical equations for the extreme closed classical trajectory (starting and ending at times $t_i^{(j)}$ and $t_r^{(j)}$) along which an electron having zero initial momentum gains the maximum classical energy, $E_{\rm cl}^{(j)}$ (cf. Ref. [15]):

$$\frac{1}{t_r - t_i}\int_{t_i}^{t_r} A(\tau)d\tau - A(t_i) = 0,$$
$$\frac{1}{c}\frac{A(t_r) - A(t_i)}{t_r - t_i} + F(t_r) = 0, \qquad (2)$$

where $\hat{\mathbf{z}}A(t)$ is the vector potential of the electric field $\mathbf{F}(t)$ [$F(t) = -(1/c)\partial A/\partial t$]. The desired solutions $(t_i^{(j)}, t_r^{(j)})$ of the system (2) are those real solutions that lie in the time interval of the jth and $(j+1)$th half-cycles, ensuring the shortest return time, $\Delta t_j = t_r^{(j)} - t_i^{(j)}$. The moment of ionization $t_i^{(j)}$ determines also an effective value of the Keldysh parameter, $\tilde{\gamma}_j$, for the jth half-cycle,

$$\tilde{\gamma}_j = \hbar\omega/(|e|\tilde{F}_j\kappa^{-1}), \quad \tilde{F}_j = |F(t_i^{(j)})|, \qquad (3)$$

where $\kappa = \sqrt{2m|E_0|}/\hbar$ and E_0 is the ground state energy of the electron: $E_0 = -\hbar^2\kappa^2/(2m)$. With known $t_i^{(j)}$ and $t_r^{(j)}$, the amplitude $\mathcal{A}_j$ can be approximated in a way similar to that for a monochromatic field [12, 20].

The resulting expression for the (dimensionless) spectral density $\rho(E_\Omega)$ can be presented in a factorized form similar to that in Refs. [12, 13, 15],

$$\rho(E_\Omega) = w(E)\sigma^{(r)}(E), \quad E = E_\Omega - |E_0|, \qquad (4)$$

where $\sigma^{(r)}(E)$ is the PRCS of an electron with momentum $\mathbf{p}$ ($p = \sqrt{2mE}$) parallel to the polarization direction $\hat{\mathbf{z}}$ of the harmonic (recombination) photon of energy E_Ω. The term $w(E)$ in Eq. (4) is the EWP, which generalizes the EWP $W(E)$ for a monochromatic field [12] to the case of a short pulse. The expression for $w(E)$ involves the sum of two terms,

$$w(E) = w_{\rm dir}(E) + w_{\rm int}(E). \qquad (5)$$

The "direct" term, $w_{\rm dir}(E)$, originates from the sum of $|\mathcal{A}_j|^2$ and involves the sum of EWPs $w_j(E)$ created during each half-cycle of the laser pulse,

$$w_{\rm dir}(E) = \sum_j w_j(E). \qquad (6)$$

The interference term in Eq. (5) originates from the interference between the half-cycle amplitudes $\mathcal{A}_j$ and $\mathcal{A}_k$ ($j \neq k$) and thus involves their phase difference:

$$w_{\rm int}(E) = \sum_{k\neq j} s_{jk}\sqrt{w_j(E)w_k(E)}\cos(\varphi_j - \varphi_k), \qquad (7)$$

where the phases φ_j and φ_k are ($l = j, k$):

$$\varphi_l = \Omega t_r^{(l)} - \frac{1}{\hbar}\int_{t_i^{(l)}}^{t_r^{(l)}} \left\{\frac{e^2}{2mc^2}[A(t_i^{(l)}) - A(\tau)]^2 - E_0\right\} d\tau.$$

The sign factor s_{jk} ($= \pm 1$) in Eq. (7) is $s_{jk} = (-1)^{j-k}\mathrm{sign}[\mathrm{Ai}(\xi_j)\mathrm{Ai}(\xi_k)]$, where $\mathrm{Ai}(\xi)$ is the Airy function [see Eq. (10)]. The half-cycle EWP $w_j(E)$ may be presented in terms of the ionization ($\mathcal{I}_j$) and propagation ($\mathcal{W}_j$) factors, which have the *same form* as for the case of a monochromatic field [12]:

$$w_j(E) = \frac{\pi\Omega}{2\omega^2}\mathcal{I}_j\mathcal{W}_j(E), \qquad (8)$$

$$\mathcal{I}_j = \frac{4\tilde{\gamma}_j^2\Gamma_{st}(\tilde{F}_j)}{(2l+1)\pi\kappa v_{\rm at}}, \quad v_{\rm at} = \frac{e^2}{\hbar}, \qquad (9)$$

$$\mathcal{W}_j(E) = \frac{p}{m}\frac{\mathrm{Ai}^2(\xi_j)}{(v_{\rm at}\Delta t_j)^3\zeta_j^{2/3}}. \qquad (10)$$

The (dimensionless) factor $\mathcal{I}_j$ involves the tunneling rate, $\Gamma_{st}(\tilde{F}_j)$, for a bound atomic electron (with energy E_0, angular momentum l, and projection $m_l = 0$) in a static electric field $\hat{\mathbf{z}}\tilde{F}_j$ [21]:

$$\Gamma_{\rm st}(\tilde{F}_j) = \frac{|E_0|}{\hbar}(2l+1)C_{\kappa l}^2\left(\frac{2F_a}{\tilde{F}_j}\right)^{2\nu-1} e^{-2F_a/(3\tilde{F}_j)}, \qquad (11)$$

where $\nu = Z/(\kappa a_0)$ (a_0 is the Bohr radius), $Z|e|$ is the charge of the remaining atomic core ($Z = 1$ for neutral atoms), $F_a = \sqrt{8m|E_0|^3}/(|e|\hbar) = (Z/\nu)^3|e|/a_0^2$, and $C_{\kappa l}$ is given by the known asymptotic form of the bound-state wave function for a Coulomb-like potential (cf. Ref. [12]).

The dimensionless parameter ζ_j and the argument ξ_j of the Airy function, $\mathrm{Ai}(\xi_j)$, in Eq. (10) for the propagation factor are given by (cf. Ref. [15]):

$$\zeta_j = \frac{I(t_r^{(j)})}{2I_{\rm at}}\left[\left|\frac{\dot{F}(t_r^{(j)})}{F(t_r^{(j)})}\right|\Delta t_j + \frac{F(t_r^{(j)})}{F(t_i^{(j)})} - 1\right], \qquad (12)$$

$$\xi_j = \frac{E - E_{\rm max}^{(j)}}{\zeta_j^{1/3}E_{\rm at}}, \qquad (13)$$

$$E_{\rm max}^{(j)} = \frac{\left[eF(t_r^{(j)})\Delta t_j\right]^2}{2m} - \frac{F(t_r^{(j)})}{F(t_i^{(j)})}|E_0|, \qquad (14)$$

where $I(t_r^{(j)}) = cF^2(t_r^{(j)})/(8\pi)$, $I_{\rm at} = 3.51\times10^{16}$ W/cm^2, and $E_{\rm at} = 27.21$ eV. Note that the first term in $E_{\rm max}^{(j)}$ is the aforementioned classical energy $E_{\rm cl}^{(j)}$, while the second term gives the quantum correction to $E_{\rm cl}^{(j)}$ [15].

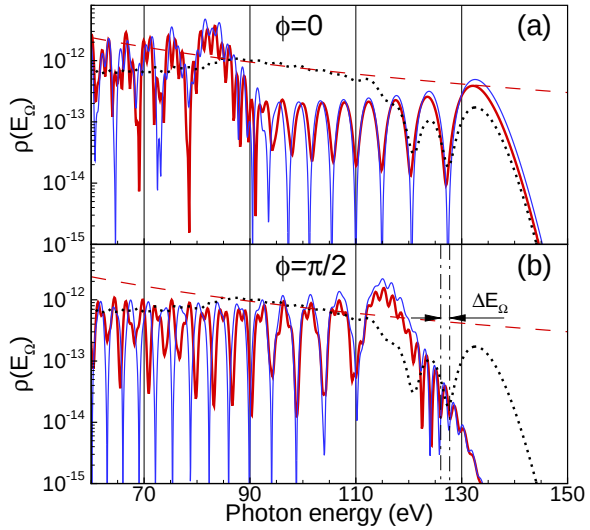

FIG. 1. (color online) The spectral densities $\rho(E_\Omega)$ for the H atom in single-cycle laser pulses [cf. Eq. (15)] with $N = 1$, $I_0 = 1.75 \times 10^{14}\,\mathrm{W/cm^2}$, $\lambda = 1.6\,\mu\mathrm{m}$, and two CEPs: (a) $\phi = 0$; (b) $\phi = \pi/2$. Thick (red) solid lines: TDSE results; thin (blue) solid lines: the result (4); dotted lines: the CEP-averaged result (4); dashed lines: $\sigma^{(r)}_{H(1s)}(E)$ (in arb. units).

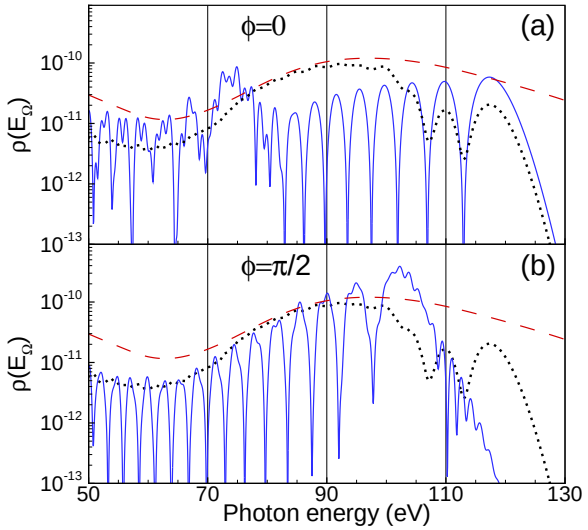

FIG. 2. (color online) The same as in Fig. 1, but for Xe with $I_0 = 1.24 \times 10^{14}\,\mathrm{W/cm^2}$ and $\lambda = 1.8\,\mu\mathrm{m}$. Dashed lines: the PRCS $\sigma^{(r)}_{\mathrm{Xe}(5p)}(E)$ deduced (using the principle of detailed balance) from the theoretical (relativistic random phase approximation) results for the photoionization cross section [23].

In Fig. 1 we compare our analytic predictions for $\rho(E_\Omega)$ with numerical TDSE results (see Ref. [15] for details of the solution of the 3D TDSE for the H atom). In order to exclude any DC component from both the electric field $F(t)$ and the vector potential $A(t)$ of the laser pulse, the pulse is parameterized using the integral,

$$\int^t A(\tau)d\tau = \frac{cF_0}{\omega^2}\mathrm{e}^{-2\ln(2)\,t^2/\tau^2}\cos(\omega t+\phi)\,, \qquad (15)$$

from which $A(t)$ and $F(t)$ can be found by differentiation. The pulse duration is $\tau = 2\pi N/\omega$, where N is the number of cycles in the full width at half-maximum. The peak intensity of the pulse is $I_0 = cF_0^2/(8\pi)$. The analytic result (4), shown in Fig. 1 for $N = 1$, is in excellent agreement with the TDSE results in the high energy plateau region. The dominant contributions to $\rho(E_\Omega)$ for a one-cycle pulse come from only *two* EWPs $w_j(E)$, one "born" near the peak of the pulse's major half-cycle and the other near the minimum of the preceding half-cycle. Only these two EWPs have substantial magnitudes of both ionization factors $\mathcal{I}_j$ [which determine the absolute value of $w_j(E)$ in Eq. (8)] and energies $E^{(j)}_{\max}$ [which determine the maximum electron energy E, beyond which the EWP $w_j(E)$ decreases exponentially, owing to the behavior of the Airy function in Eq. (10)].

Our theory provides a clear explanation (that agrees with previous numerical findings [3, 5, 8–10]) for the strong CEP-dependence of $\rho(E_\Omega)$. In particular, the two-plateau structure of the spectrum for $\phi = 0$ and its disappearance for $\phi = \pi/2$ originates from the strong CEP-dependence of the "cutoff energies" $E^{(j)}_{\mathrm{cut}}$ for two contributing half-cycle amplitudes $\mathcal{A}_j$. (These energies are 136.5 and 85.7 eV for $\phi = 0$ and 129.3 and 118.7 eV for $\phi = \pi/2$.) The large-scale oscillations in Fig. 1 originate from the interference of two (short and long) electron trajectories that contribute to the half-cycle amplitudes $\mathcal{A}_j$ and thus to the EWPs $w_j(E)$. These oscillations are similar to those for a monochromatic field [20] and are described by the Airy function in Eq. (10) [22], i.e., they are unrelated to the interference between subcycle amplitudes $\mathcal{A}_j$. The latter interference produces another feature that occurs only for non-monochromatic pulses and disappears upon omitting the term $w_{\mathrm{int}}(E)$ in Eq. (5): the fine-scale modulation of $\rho(E_\Omega)$ visible in Figs. 1(a,b) in regions where the two half-cycle amplitudes $\mathcal{A}_j$ interfere. From the explicit form of $w_{\mathrm{int}}(E)$ (7), one obtains the interval ΔE_Ω [cf. Fig. 1(b)] between two sequential fine-scale maxima/minima in $\rho(E_\Omega)$ as (cf. Ref. [6]):

$$\Delta E_\Omega = 2\pi\hbar/\Delta t_r = \mathcal{C}\hbar\omega, \qquad (16)$$

where $\Delta t_r = t_r^{(j+1)} - t_r^{(j)}$ and the constant $\mathcal{C}$ ($1 \lesssim \mathcal{C} \lesssim 2$) is sensitive to the pulse shape.

Figure 2 shows single-cycle results for $\rho(E_\Omega)$ of Xe for pulse parameters F_0 and ω in Eq. (15) such that $(\hbar\omega/|E_0|)_{\mathrm{H}} = (\hbar\omega/|E_0|)_{\mathrm{Xe}}$ and $F_0^{\mathrm{H}}/F_0^{\mathrm{Xe}} = r^{3/2}$ (where $r \equiv |E_0^{\mathrm{H}}/E_0^{\mathrm{Xe}}| = 1.12$), which facilitates comparison with $\rho(E_\Omega)$ of H in Fig. 1. With these parameters, the EWPs for H and Xe coincide upon multiplying the latter by the ratio of asymptotic coefficients, $(C^{\mathrm{H}}_{\kappa l}/C^{\mathrm{Xe}}_{\kappa l})^2 \approx 0.65$, and re-scaling the electron and harmonic energies for Xe according to $E\,(E_\Omega) \to rE\,(E_\Omega)$. Thus, differences between Figs. 1 and 2 originate entirely from the PRCSs: $\sigma^{(r)}_{H(1s)}(E)$ is flat whereas $\sigma^{(r)}_{\mathrm{Xe}(5p)}(E)$ exhibits a resonance-like feature, caused by many-electron correlations involv-

ing the Xe $4d$-subshell [23]. Fig. 2 predicts such atom-specific dynamical features (whose occurrence in HHG by long pulses was discussed recently in Refs. [12, 15, 16]) to occur also in single-cycle HHG spectra. Moreover, Fig. 2 predicts that the CEP can be used to modify their magnitudes and shapes as compared to the CEP-averaged results for $\rho(E_\Omega)$ (cf. $E_\Omega \approx$ 100-110 eV).

As the number, N, of optical cycles increases, more than two amplitudes $\mathcal{A}_j$ contribute to the HHG spectrum, thus leading to marked differences from the case $N = 1$. First, already for $N = 2$, the two-plateau structure of $\rho(E_\Omega)$ for $\varphi = 0$ disappears and our results for this case are similar to the TDSE results for the H atom in Ref. [3]. Second, the fine-scale modulation resulting from many interfering amplitudes $\mathcal{A}_j$ becomes much more pronounced, leading to a CEP-sensitive "harmonic structure" in the cutoff region and beyond. The positions of these harmonics are different for sine and cosine pulses and (for both cases) do not coincide with the position of odd harmonics of the carrier frequency: $E_\Omega = (2k+1)\hbar\omega$ (cf. Refs. [3, 5, 6]). Our analysis shows that for a Gaussian pulse these latter harmonics start to form in the cutoff region only for pulses with $N \gtrsim 10$, while for a trapezoidal pulse they appear already for $N = 3$.

The evolution of $\rho(E_\Omega)$ (4) as a pulse becomes long is most easily derived for a flat-top (trapezoidal) pulse with n half-cycles. For such a pulse, the times $t_i^{(j)}$ and $t_r^{(j)}$ for neighboring half-cycles differ by π/ω, so that the EWPs w_j become the same for any j, while the factor s_{jk} and the phase difference in Eq. (7) reduce to $s_{jk} = (-1)^{j-k}$ and $\varphi_j - \varphi_k = \pi(j-k)E_\Omega/(\hbar\omega)$. Calculating the sum of $w_{\rm dir}$ and $w_{\rm int}$ in Eq. (5) analytically, we find:

$$\rho(E_\Omega) = \frac{\pi\Omega}{2\omega^2} W(E)\sigma(E)D(n,\Omega),$$
$$D(n,\Omega) = \frac{\sin^2\left[\frac{\pi n}{2}\left(\frac{\Omega}{\omega}+1\right)\right]}{\sin^2\left[\frac{\pi}{2}\left(\frac{\Omega}{\omega}+1\right)\right]}, \qquad (17)$$

where $W(E)$ is the EWP for a monochromatic pulse [12], while the factor $D(n,\Omega)$ ensures the $2\hbar\omega$-spacing of the HHG spectrum for a monochromatic field: For $n \to \infty$,

$$D(n,\Omega) \approx \frac{2\omega^2}{\pi} T_n \sum_k \delta[\Omega - (2k+1)\omega], \quad T_n = \pi n/\omega.$$

To conclude, we have derived quantum-mechanically a factorized formula (4) for the high-energy part of the spectral density $\rho(E_\Omega)$ that is valid for a short laser pulse of any shape. It predicts the existence of atom-specific, many-electron dynamical features in HHG spectra for even a one-cycle pulse and strong modification of these features by CEP effects. It predicts also significant pulse shape dependence for the evolution of HHG spectra with increasing number of optical cycles. To apply our analytic results, only the PRCS $\sigma^{(r)}(E)$ for the target atom and the solutions $(t_i^{(j)}, t_r^{(j)})$ of the classical equations (2) for a given short pulse are needed. Our results agree with numerical TDSE results and provide an efficient tool for analyses of HHG by few-cycle laser pulses.

This work was supported by RFBR Grants 10-02-00235 and 10-02-01250, by NSF Grant PHY-0901673, by Grant MK-2425.2009.2 (M.V.F) of the President of the RF, and by the "Dynasty" Foundation (A.A.S).

[1] T. Brabec and F. Krausz, Rev. Mod. Phys. **72**, 545 (2000); F. Krausz and M. Ivanov, *ibid.* **81**, 163 (2009).
[2] K.J. Schafer, B. Yang, L.F. DiMauro, and K.C. Kulander, Phys. Rev. Lett. **70**, 1599 (1993); P.B. Corkum, *ibid.* **71**, 1994 (1993).
[3] A. de Bohan, P. Antoine, D.B. Milošević, and B. Piraux, Phys. Rev. Lett. **81**, 1837 (1998).
[4] A. Baltuška *et al.*, Nature (London) **421**, 611 (2003).
[5] V.S. Yakovlev and A. Scrinzi, Phys. Rev. Lett. **91**, 153901 (2003).
[6] M. Nisoli *et al.*, Phys. Rev. Lett. **91**, 213905 (2003).
[7] C.A. Haworth *et al.*, Nat. Phys. **3**, 52 (2007).
[8] A.D. Bandrauk, S. Chelkowski, D.J. Diestler, J. Manz, and K.J. Yuan, Phys. Rev. A **79**, 023403 (2009).
[9] P. Huang, X.T. Xie, X. Lü, J. Li, and X. Yang, Phys. Rev. A **79**, 043806 (2009).
[10] G. Sansone *et al.*, Phys. Rev. A **80**, 063837 (2009).
[11] M. Lewenstein, Ph. Balcou, M.Y. Ivanov, A. L'Huillier, and P.B. Corkum, Phys. Rev. A **49**, 2117 (1994).
[12] M.V. Frolov *et al.*, Phys. Rev. Lett. **102**, 243901 (2009).
[13] T. Morishita, A.T. Le, Z. Chen, and C.D. Lin, Phys. Rev. Lett. **100**, 013903 (2008); C.D. Lin *et al.*, J. Phys. B **43**, 122001 (2010).
[14] S. Minemoto *et al.*, Phys. Rev. A **78**, 061402(R) (2008); H.J. Wörner, H. Niikura, J.B. Bertrand, P.B. Corkum, and D.M. Villeneuve, Phys. Rev. Lett. **102**, 103901 (2009).
[15] M.V. Frolov, N.L. Manakov, A. A. Silaev, and N. V. Vvedenskii, Phys. Rev. A **81**, 063407 (2010).
[16] M.V. Frolov, N.L. Manakov, and A.F. Starace, Phys. Rev. A **82**, 023424 (2010).
[17] M.V. Frolov, A.V. Flegel, N.L. Manakov, and A.F. Starace, Phys. Rev. A **75**, 063407 (2007).
[18] N.L. Manakov, V.D. Ovsiannikov, and L.P. Rapoport, Phys. Rep. **141**, 319 (1986).
[19] M.V. Frolov, A.V. Flegel, N.L. Manakov, and A.F. Starace, Phys. Rev. A **75**, 063408 (2007).
[20] M.V. Frolov, N.L. Manakov, T.S. Sarantseva, and A.F.

Starace, J. Phys. B **42**, 035601 (2009).
[21] B.M. Smirnov and M.I. Chibisov, Zh. Eksp. Teor. Fiz. **49**, 841 (1965) [Sov. Phys. JETP **22**, 585 (1966)].
[22] The large-scale oscillations scale with I_0 as $\sim I_0^{1/3}$ [20].
[23] M. Kutzner, V. Radojević, and H.P. Kelly, Phys. Rev. A **40**, 5052 (1989).